

# Real-time Musical Score Following from a Live Audio Source

*Andrew Lee  
Maneesh Agrawala, Ed.  
Carlo H. Séquin, Ed.*



Electrical Engineering and Computer Sciences  
University of California at Berkeley

Technical Report No. UCB/EECS-2014-127

<http://www.eecs.berkeley.edu/Pubs/TechRpts/2014/EECS-2014-127.html>

May 22, 2014

Copyright © 2014, by the author(s).  
All rights reserved.

Permission to make digital or hard copies of all or part of this work for personal or classroom use is granted without fee provided that copies are not made or distributed for profit or commercial advantage and that copies bear this notice and the full citation on the first page. To copy otherwise, to republish, to post on servers or to redistribute to lists, requires prior specific permission.

### Acknowledgement

I thank the Electrical Engineering and Computer Sciences department at UC Berkeley for funding my Masters year. I would like to thank my research advisor Maneesh Agrawala and my reader Carlo Séquin for all of their help and guidance during my graduate education. The work described in this paper was done in the context of the final project for the UC Berkeley course User Interface Design and Development, and I would like to thank Maneesh Agrawala and Björn Hartmann for teaching it. Finally, I would like to thank my family and friends for supporting me throughout the year.

---

**Real-time Musical Score Following from a Live Audio Source**

by Andrew Lee

---

**Research Project**

Submitted to the Department of Electrical Engineering and Computer Sciences,  
University of California at Berkeley, in partial satisfaction of the requirements for  
the degree of **Master of Science, Plan II.**

Approval for the Report and Comprehensive Examination:

**Committee:**

---

Professor Maneesh Agrawala  
Research Advisor

---

(Date)

\* \* \* \* \*

---

Professor Carlo H. Séquin  
Second Reader

---

(Date)

# Acknowledgments

I thank the Electrical Engineering and Computer Sciences department at UC Berkeley for funding my Masters year.

I would like to thank my research advisor Maneesh Agrawala and my reader Carlo Séquin for all of their help and guidance during my graduate education.

The work described in this paper was done in the context of the final project for the UC Berkeley course *User Interface Design and Development*, and I would like to thank Maneesh Agrawala and Björn Hartmann for teaching it.

Finally, I would like to thank my family and friends for supporting me throughout the year.

# Abstract

Musical score following has many practical applications. As mobile devices get more popular, musicians would like to carry their sheet music on their mobile devices. One useful functionality that a sheet music app could offer is to have the app follow the music being played by the musician and turn pages at the right time. In this paper, we describe how we combined several techniques to accomplish this task and how we implemented it to run efficiently. By understanding basic sheet music semantics and how instruments produce sound, we carefully constructed a hidden Markov model to follow a player's position in a musical score solely by listening to their playing. We implemented our algorithm in Java, in the form of a sheet music application for Android, and it was able to successfully follow amateur-level pianists playing *Twinkle Twinkle Little Star*, as well as *Minuet in G*, by J.S. Bach.

# Contents

|          |                                                      |           |
|----------|------------------------------------------------------|-----------|
| <b>1</b> | <b>Introduction</b>                                  | <b>6</b>  |
| <b>2</b> | <b>Related Work</b>                                  | <b>7</b>  |
| <b>3</b> | <b>Algorithm</b>                                     | <b>8</b>  |
| 3.1      | Hidden Markov Model Formulation . . . . .            | 8         |
| 3.1.1    | The Hidden State . . . . .                           | 8         |
| 3.1.2    | The Observable State . . . . .                       | 10        |
| 3.1.3    | Using the Forward Algorithm . . . . .                | 10        |
| 3.2      | Designing the Emission Distributions . . . . .       | 11        |
| 3.2.1    | Musical Note Mechanics . . . . .                     | 11        |
| 3.2.2    | Probability Computation . . . . .                    | 13        |
| 3.3      | Designing the Transition Probabilities . . . . .     | 14        |
| 3.3.1    | Restricting Transitions by Page . . . . .            | 16        |
| <b>4</b> | <b>Implementation</b>                                | <b>17</b> |
| 4.1      | Goertzel Algorithm . . . . .                         | 17        |
| 4.2      | Preprocessing . . . . .                              | 18        |
| 4.3      | Main Loop . . . . .                                  | 18        |
| 4.4      | Restricting the Considered States . . . . .          | 19        |
| 4.5      | Results . . . . .                                    | 19        |
| <b>5</b> | <b>Future Work</b>                                   | <b>22</b> |
| 5.1      | Understanding Tempo and Rhythm . . . . .             | 22        |
| 5.2      | Extension to other Instruments . . . . .             | 22        |
| 5.3      | Better Note Break Detection . . . . .                | 23        |
| 5.4      | Additional Considerations for a Useful App . . . . . | 23        |
| 5.4.1    | Importing Sheet Music . . . . .                      | 23        |
| 5.4.2    | Pagination and Page Transitions . . . . .            | 23        |
| <b>6</b> | <b>Summary</b>                                       | <b>25</b> |
| <b>A</b> | <b>Observed Frequencies Table</b>                    | <b>27</b> |

|                                                                                  |           |
|----------------------------------------------------------------------------------|-----------|
| <b>B Computing <math>N</math> and <math>k</math> for each Observed Frequency</b> | <b>30</b> |
| <b>C <i>Minuet in G</i> Note Sets</b>                                            | <b>31</b> |

# Chapter 1

## Introduction

Many piano players who use sheet music understand the annoyance of having to flip pages. In a live performance, it is common to hire another person whose only task is to turn pages for the performer. Otherwise, the piano player has to turn the pages themselves, which requires taking their hand off the keyboard, causing a disruption in their playing. Recently, some electronic products have emerged that allow hands-free page turning for both physical and digital sheet music. However, they are usually foot-operated, so the pianist still needs to execute a conscious action to flip the page.

We set out to create a mobile app that automatically advances pages for the player as they play, never requiring them to perform any action outside of simply playing their piece. In other words, we want to digitally replicate the job of the human page turner. This required a method to understand where in the score the player is playing so we know when the player has reached the end of the page. Additionally, to make it work on regular acoustic pianos without any special apparatus, we do not have the luxury of technologies like MIDI to directly measure what keys the user is playing, so the only source of input we employ is sound. It is this method which we will describe in this paper. Using a hidden Markov model with carefully designed probabilities, we have developed an algorithm that can follow a player's piano playing after being given the musical score. Our algorithm has been fully realized in the form of a sheet music application for Android.

## Chapter 2

# Related Work

Our problem belongs to a field known as musical score following, which aims to find a correspondence between a known musical score and a performance of that piece. In this field, the problems can be categorized into two types: off-line and on-line. In the off-line case, which is sometimes called score matching, the performance in its entirety has already been recorded, and thus, the approaches to this problem have the ability to “look into the future” to better establish the correspondence. The on-line case does not have this luxury, as its task is to continuously find this correspondence in real-time as the performer plays.

One class of approaches is based on dynamic time warping. As its name suggests, the goal is to warp sequences in time to find a way to make them match. While its usefulness is evident in an off-line setting, it is not as clear in an on-line setting, since the performance in the future is not available. Work has been done to adapt dynamic time warping for streaming data [5, 6].

One of the most popular techniques to score following is to employ a hidden Markov model [4]. While the specifics vary by approach, most define the hidden states in terms of the notes in the original score and have the observable states correspond to the audio that is produced by those notes [8–10].

# Chapter 3

## Algorithm

Our goal is to infer where the player is currently playing within sheet music. While we cannot directly measure where in the piece the player is consciously playing, we can indeed observe the sounds that they produce using the piano. Formulating the problem in this manner naturally lends itself to an application of the hidden Markov model.

### 3.1 Hidden Markov Model Formulation

To model our problem as a hidden Markov model, we need to define the hidden states and the observable states.

#### 3.1.1 The Hidden State

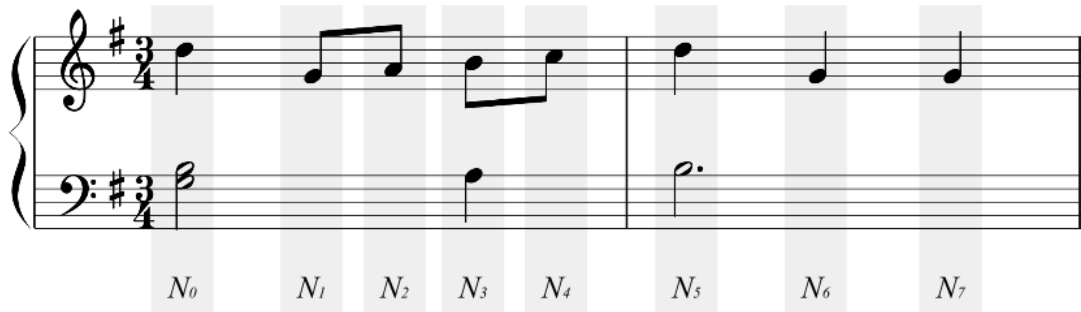
At a high level, we define the hidden state to be the player’s position in the piece. Specifically, we define each state as a set of notes, which we aptly call a **note set**. When a given state is active, that means the notes in that state are currently being emitted from the instrument.

The first step in determining our set of possible states is to generate a sequence of note sets  $\{N_0, N_1, N_2, \dots\}$  by creating one at every onset of new notes in the score. Figure 3.1a depicts an example of how we do this.

Notice that for sections where a note is being held while new notes are being played, we only consider the new notes for each note set. The reason we disregard the note after its original onset is because by the time the new notes are played, the sound of the former may have died down and become overshadowed by the latter.

If there are repeats or other control flow notations in the sheet music such as *D.C. al Fine*, we “unfold” them beforehand, so that the sequence of note sets  $N_i$  is just a simple linear representation of the notes in the score, in the order that the player will play them. Thus, as the player progresses through the music, they would keep jumping to the following state as they play the notes.

We found that these  $N_i$  note sets alone were insufficient for our needs. This rudimentary formulation assumes that the player is playing something at all times, and does not accommodate the case when the player is at rest. To remedy this, we artificially create a note set  $R_i$  to follow each  $N_i$ . Every  $R_i$  is an empty set, which represents the state of playing no notes. Semantically, if the player is currently at  $R_i$ , which we



(a) Determining note sets  $N_i$  from the sheet music.

$$\begin{aligned}
 S^0 &= N_0 = \{G_3, B_3, D_5\} \\
 S^1 &= R_0 = \{\} \\
 S^2 &= N_1 = \{G_4\} \\
 S^3 &= R_1 = \{\} \\
 S^4 &= N_2 = \{A_4\} \\
 S^5 &= R_2 = \{\} \\
 S^6 &= N_3 = \{A_3, B_4\} \\
 S^7 &= R_3 = \{\} \\
 S^8 &= N_4 = \{C_5\} \\
 S^9 &= R_4 = \{\} \\
 S^{10} &= N_5 = \{B_3, D_5\} \\
 S^{11} &= R_5 = \{\} \\
 S^{12} &= N_6 = \{G_4\} \\
 S^{13} &= R_6 = \{\} \\
 S^{14} &= N_7 = \{G_4\} \\
 S^{15} &= R_7 = \{\}
 \end{aligned}$$

(b) Defining the list of states  $S^k$ , using the original note sets  $N_i$  and the artificially created note sets  $R_i$ .

Figure 3.1: The first two measures of J.S. Bach's *Minuet in G* converted into note sets, and then defined into the hidden states.

call the **rest state** of  $N_i$ , that means they have stopped playing state  $N_i$ , or that they have held out the notes in state  $N_i$  so long that the background noise overtakes the signal of the notes. Either way, it acts as a holdover state while the player has not yet advanced to playing state  $N_{i+1}$ .

Now, we have finished defining the set of all possible states. For notation purposes, we will define  $S^i$  as the following:

$$S^i = \begin{cases} N_{\frac{i}{2}} & \text{if } i \text{ is even} \\ R_{\frac{i-1}{2}} & \text{if } i \text{ is odd} \end{cases}$$

In other words,  $\{S^0, S^1, S^2, S^3, \dots\}$  is the sequence of  $N_i$  interleaved with the sequence of  $R_i$ . Figure 3.1b shows the result of this process, continuing the previous example.

### 3.1.2 The Observable State

At a high level, the observable state is the sound that is produced by the notes in a note set. Specifically, we define the observable state to be a vector of 88 real values, which correspond to the magnitudes of 88 particular frequencies emitted by the notes being played. We call this vector the **magnitude vector**, which we denote as  $\mathbf{m}$ . The 88 frequencies whose magnitudes we are interested in are the 88 fundamental frequencies of the keys on a full piano keyboard, from 27.5 Hz ( $A_0$ ) to 4186.01 Hz ( $C_8$ ), as listed in Table A.1. We will call these 88 frequencies the **observed frequencies**. The idea is that using a model of how instruments produce sound, we can predict how loud each of the observed frequencies will be when a note set is played.

### 3.1.3 Using the Forward Algorithm

Because we will be performing the inference in real-time, and thus have no access to audio in the future, we will only use the forward algorithm to compute the likelihoods of the hidden states. The canonical form of the forward algorithm is written as:

$$p(S_t, \mathbf{m}_{1:t}) = p(\mathbf{m}_t | S_t) \sum_{S_{t-1}} p(S_t | S_{t-1}) p(S_{t-1}, \mathbf{m}_{1:t-1})$$

$S_t$  and  $\mathbf{m}_t$  represent the state and magnitude vector at time  $t$ , respectively. We use the notation  $\mathbf{m}_{1:t}$  to denote the sequence of magnitude vectors from time 1 to  $t$ . This means that  $p(S_t, \mathbf{m}_{1:t})$  represents the probability of observing the sequence  $\mathbf{m}_{1:t}$  and that the current state is  $S_t$ .  $p(\mathbf{m}_t | S_t)$  represents the emission probability, or how likely the magnitude vector  $\mathbf{m}_t$  could have been emitted from state  $S_t$ .  $p(S_t | S_{t-1})$  represents the transition probability, or the probability that the current state is  $S_t$  given that the previous state was  $S_{t-1}$ . Basically, this equation tells us how to update the value  $p(S_t, \mathbf{m}_{1:t})$  for every state  $S_t$  when a new observed state  $\mathbf{m}_t$  comes in.

However, we do not really care about the joint probabilities of the current hidden state with the sequence of observed states. Rather, we are interested in the probabilities of the current hidden state *given* the sequence of observed states thus far. This is called the filtering form of the forward algorithm, which can be expressed as:

$$p(S_t|\mathbf{m}_{1:t}) \propto p(\mathbf{m}_t|S_t) \sum_{S_{t-1}} p(S_t|S_{t-1})p(S_{t-1}|\mathbf{m}_{1:t-1})$$

This form lets us renormalize the probabilities at the end after computing the sums for each possible state. One of the great advantages of this normalization is that we can be more relaxed in the design of our emission probability distribution,  $p(\mathbf{m}_t|S_t)$ . Ultimately, the property that we want  $p(\mathbf{m}_t|S_t)$  to have is that given  $\mathbf{m}_t$ , if we believe state  $S^i$  is more likely than  $S^j$  to have emitted  $\mathbf{m}_t$ , then  $p(\mathbf{m}_t|S^i) > p(\mathbf{m}_t|S^j)$ . Rather than designing  $p(\mathbf{m}_t|S_t)$  such that it obeys the required probability properties, we can instead design a function  $E$  that has the property, if state  $S^i$  is more likely to have produced  $\mathbf{m}_t$  than state  $S^j$ , then  $E(\mathbf{m}_t, S^i) > E(\mathbf{m}_t, S^j)$ . Thus, our update equation can be rewritten as:

$$p(S_t|\mathbf{m}_{1:t}) \propto E(\mathbf{m}_t, S_t) \sum_{S_{t-1}} p(S_t|S_{t-1})p(S_{t-1}|\mathbf{m}_{1:t-1})$$

## 3.2 Designing the Emission Distributions

To design a good emission distribution, we need to first understand what happens when notes are played on the piano.

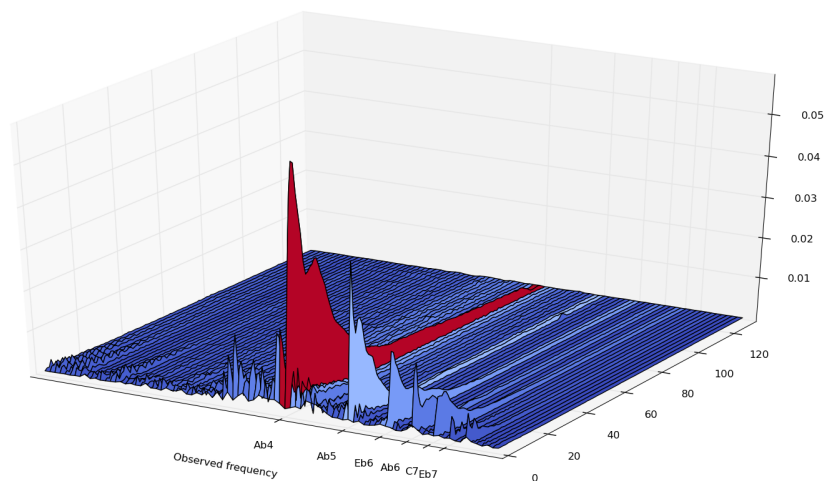
### 3.2.1 Musical Note Mechanics

A string with fixed ends has multiple frequencies that it can resonate at, called harmonics. We often call the lowest harmonic the fundamental frequency (the one we perceive as the pitch of the note) and the other ones overtones. If the string is ideal, the overtones exist at integer multiples of the fundamental. While a real string's overtones do not exactly correspond to integer multiples of its fundamental frequency (they are typically slightly higher), in this application, they are close enough that we treat them as such.

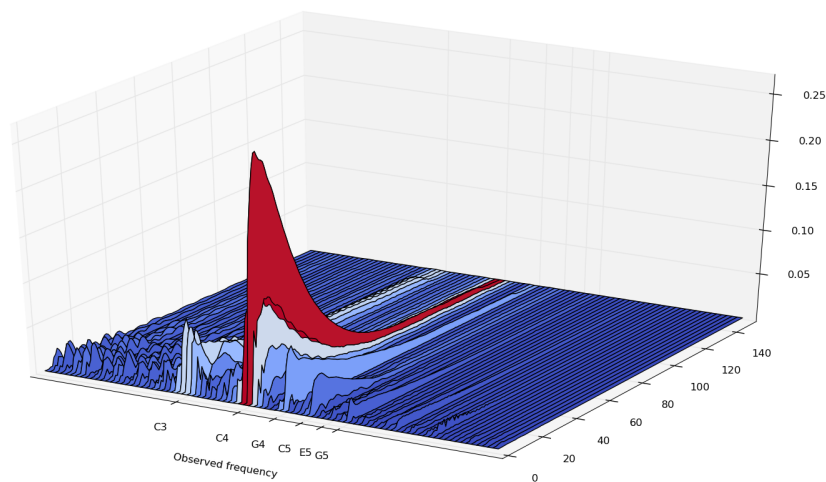
Since the frequencies of the notes on a musical scale increase exponentially, while the harmonics are spaced linearly in frequency, the overtones of a note actually space out in a logarithmic fashion. Musically speaking, the first five overtones of a note occur roughly 12, 19, 24, 28, and 31 semitones above that note.

The important aspect is that when a string is struck, which is what happens inside a piano, multiple harmonics of the string simultaneously ring out. Therefore, the sound that is produced contains not just the fundamental frequency, but the overtones as well. It is the combination of these harmonics that characterize the sound of an instrument, which we also call the timbre of the instrument.

Figure 3.2 depicts an  $A\flat_4$  note and a  $C_3$  note being played on a piano. The sound was decomposed into the observed frequencies, which the left axis represents. The right axis represents time, and the vertical axis represents the magnitudes of the frequencies over time. As predicted, there are strong magnitudes at the fundamental frequency as well as its overtones. Of course, we see that the magnitudes decay over time as the note's sound dies out. Interestingly, we observe that the magnitudes of the frequencies all decay roughly at the same proportional rate. Also, we notice that whereas the  $A\flat_4$  note's first harmonic is dominant, the second harmonic is the dominant one for the  $C_3$  note. As such, we learned that the harmonic ratios are different depending on the note.



(a) An  $A\flat_4$  note.



(b) A  $C_3$  note.

Figure 3.2: The magnitudes of the frequencies present in notes played on a piano.

Additionally, when multiple notes are played simultaneously, the resulting set of frequencies is observed to be equivalent to superposing the frequencies produced by those notes individually.

Using these observations, we decided to characterize note sets by the ratio of the strengths of the harmonic frequencies they exhibit. Using the  $A\flat_4$  note as an example, we can say that it is characterized with having frequencies at  $A\flat_4$ ,  $A\flat_5$ ,  $E\flat_6$ ,  $A\flat_6$ ,  $C_7$ , and  $E\flat_7$ , where their magnitudes obey a ratio of roughly  $10 : 6 : 3 : 3 : 2 : 1$ . Apart from background noise, this characterization is agnostic to the loudness of the note(s) at any point in its duration. In the case of a note set where multiple notes are being played at the same time, we assume that they are played at the same volume, so we construct the note set’s characteristic harmonics by simply adding together the harmonic characteristics of the component notes. Even though it is possible for the player to play the notes at different volumes, this does not happen often and we found that our algorithm still performs well when they do.

### 3.2.2 Probability Computation

Because we characterize note sets by the ratios of the magnitudes of the harmonic frequencies, we encode this description in the form of an 88-dimensional vector. A vector is a convenient form to encode this information since no matter how it is uniformly scaled, its components will all remain in the same ratio.

First, we need to determine the first six harmonic magnitudes for each note played on a piano, with each note played at the same volume. This was done empirically on a number of notes, and then interpolated for the remaining ones. The values we settled on are listed in Table A.1.

Next, we will define the vector for any note  $n$ , which we denote  $\mathbf{n}$ . Let  $\mathbf{n} = \langle n_0, n_1, n_2, \dots, n_{87} \rangle$ . If  $h_1, h_2, h_3, h_4, h_5$ , and  $h_6$  are the first six harmonic magnitudes of  $n$  and the note index of  $n$  is  $i$ , then  $n_i = h_1$ ,  $n_{i+12} = h_2$ ,  $n_{i+19} = h_3$ ,  $n_{i+24} = h_4$ ,  $n_{i+28} = h_5$ , and  $n_{i+31} = h_6$ . The remaining components are 0. Thus,  $\mathbf{n}$  is more or less the magnitude vector we would expect from playing the note  $n$ .

Consequently, we define the vector of a note set  $S$ , which we denote  $\mathbf{S}$ , as simply the vector sum of its notes’ vectors. To account for background noise, we also add a vector  $\mathbf{b}$ , which represents the magnitude vector caused by background noise. Thus, we have:

$$\mathbf{S} = \mathbf{b} + \sum_{n \in S} \mathbf{n}$$

Finally, we normalize these note set vectors, denoting them as  $\hat{\mathbf{S}}$ :

$$\hat{\mathbf{S}} = \frac{\mathbf{S}}{\|\mathbf{S}\|}$$

When the incoming sound comes in, we extract the current magnitude vector  $\mathbf{m}_t$  from the signal using the Goertzel algorithm, which is elaborated upon in Section 4.1. Then, our goal is to compare  $\mathbf{m}_t$  to the unit vectors of each possible note set  $\hat{\mathbf{S}}^i$ . Geometrically, the closer the ratio of the components in  $\mathbf{m}_t$  is to that of  $\hat{\mathbf{S}}^i$ , the more parallel the vectors are. Thus, to measure this notion, we use the dot product.  $\mathbf{m}_t \cdot \hat{\mathbf{S}}^i = \|\mathbf{m}_t\| \|\hat{\mathbf{S}}^i\| \cos \theta$ , where  $\theta$  is the angle between the two vectors. Since  $\hat{\mathbf{S}}^i$  is a unit vector, the expression reduces to  $\|\mathbf{m}_t\| \cos \theta$ , meaning that only  $\theta$  has any effect on the value. That means the dot product is greater the more parallel  $\mathbf{m}_t$  is to  $\hat{\mathbf{S}}^i$ , which is exactly what we wanted.

As mentioned in Section 3.1.3, we wish to define an emission function  $E$  that behaves like  $p(\mathbf{m}_t | S_t)$ .

Intuitively, we want  $E(\mathbf{m}_t, S_t)$  to be greater if we believe that note set  $S_t$  is more likely to produce  $\mathbf{m}_t$ . Thus, one way to define  $E$  is:

$$E(\mathbf{m}_t, S_t) = \mathbf{m}_t \cdot \hat{\mathbf{S}}_t$$

However, we found that this function was not discriminating enough. To exaggerate the differences between the regular dot product results, we square them:

$$E(\mathbf{m}_t, S_t) = (\mathbf{m}_t \cdot \hat{\mathbf{S}}_t)^2$$

We found that using higher exponents would make it too strict, so we settled on taking the square.

### 3.3 Designing the Transition Probabilities

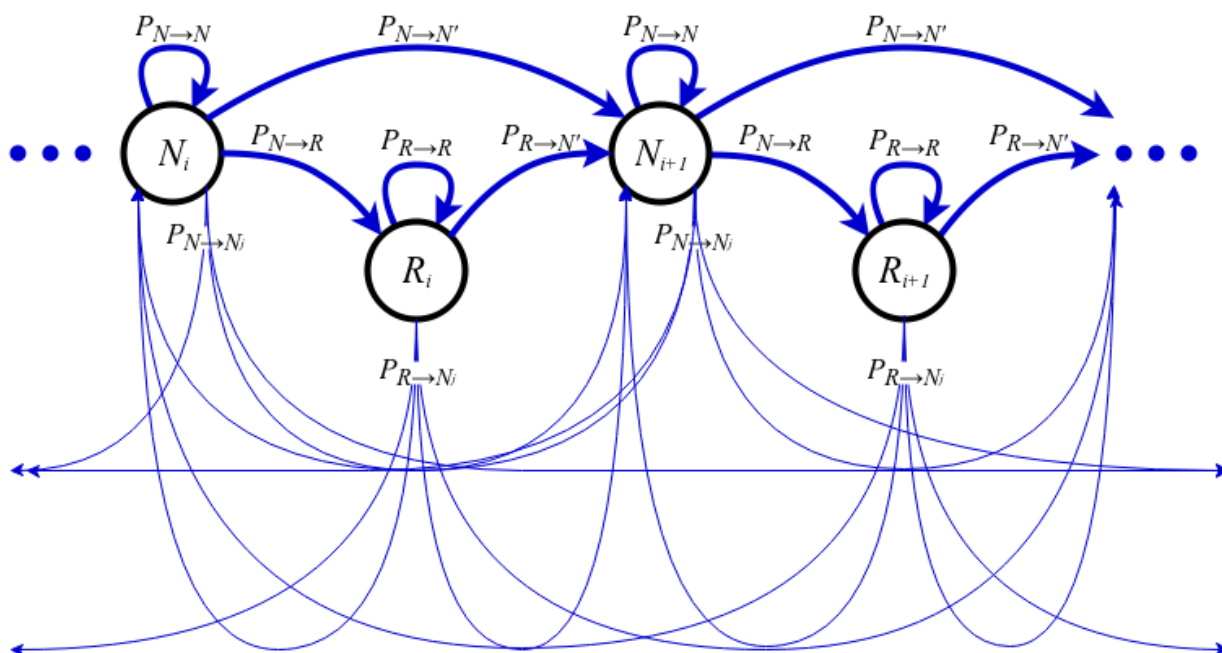


Figure 3.3: A partial sequence of note sets, along with arrows representing transition probabilities.

Figure 3.3 depicts a representative section of our hidden states. It shows arrows representing the transitions from state to state, labeled with weights. The transition types and their descriptions are as follows:

- $N_i \rightarrow N_i$ : Staying on the current note set. Considering that we will be processing audio chunks many times a second, the player will likely be holding out a note set for several cycles, so this transition accounts for that. The associated weight is  $P_{N \rightarrow N}$ .
- $N_i \rightarrow N_{i+1}$ : Advancing from the current note set to the next note set. This is the transition when the player plays the next note set. The associated weight is  $P_{N \rightarrow N'}$ .

- $N_i \rightarrow R_i$ : Advancing to the rest state of the current note set. This is transition when the signal from current note set dies out. The associated weight is  $P_{N \rightarrow R}$ .
- $N_i \rightarrow N_j$ : Jumping to note set  $N_j$  from the current note set. This is the transition when the player decides to jump to a different part of the music while playing. The associated weight is  $P_{N \rightarrow N_j}$ .
- $R_i \rightarrow R_i$ : Staying on the current rest state. Similarly, the player could spend multiple cycles playing nothing, so we need this to be able to transition to itself. The associated weight is  $P_{R \rightarrow R}$ .
- $R_i \rightarrow N_{i+1}$ : Advancing from the rest state to the next note set. This is the transition when the player plays the next note set after a period of rest. The associated weight is  $P_{R \rightarrow N'}$ .
- $R_i \rightarrow N_j$ : Jumping to note set  $N_j$  from the current rest state. This is the transition when the player decides to jump to a different part of the music while at rest. The associated weight is  $P_{R \rightarrow N_j}$ .

To compute the transition probability from state  $A$  to state  $B$ , we take the fraction of the weight of the transition from  $A$  to  $B$  over the sum of the weights of the arrows stemming from  $A$ . In other words:

$$p(B|A) = \frac{P_{A \rightarrow B}}{\sum_s P_{A \rightarrow s}}$$

Now, we will assign values to these weights. Notice that for the most part, the transitions are all about advancing along the score. The transitions  $N_i \rightarrow N_j$  and  $R_i \rightarrow N_j$ , on the other hand, allow the hidden Markov model to accommodate the user jumping around the music. Since these are a lot less common, the corresponding weights for these two will be much less.

Another consideration is what happens when the user decides to jump to a sequence of notes that happens to repeat elsewhere in the score. Our heuristic would be to place greater weight on the first instance of that sequence. To bias our model that way, we skew the values of  $P_{N \rightarrow N_j}$  and  $P_{R \rightarrow N_j}$  such that they are greater when  $j$  is lower.

After experimentation, we settled on assigning the following values:

- $P_{N \rightarrow N} = 100000$
- $P_{N \rightarrow N'} = 100000$
- $P_{N \rightarrow R} = 100000$
- $P_{N \rightarrow N_j} = 0.1^j$
- $P_{R \rightarrow R} = 100000$
- $P_{R \rightarrow N'} = 100000$
- $P_{R \rightarrow N_j} = 0.1^j$

### 3.3.1 Restricting Transitions by Page

In the context of a piece with multiple pages of sheet music, it is reasonable to believe that the player will not suddenly decide to play notes that are more than a few measures before and after the visible page. As such, we can adapt the transition probabilities accordingly.

Namely, if  $S^i$  is more than a few measures before the end of the previous page, or is more than a few measures after the start of the next page, we set the weight of all transitions pointing to  $S^i$  to 0. In other words, these states become considered unreachable. Note that these weight modifications are dependent on which page is the current one, so when the page gets flipped (either automatically or by the player), we restore the original weights, determine which states are now unreachable, and then zero out the transitions to those states.

## Chapter 4

# Implementation

We implemented this algorithm in Java for the Android platform as part of a sheet music application. We used the TarsosDSP library [12], which offered a clean framework for audio processing in Java. However, TarsosDSP depends on some Java libraries (namely, `javax` libraries) that are not available in Android, so we took out the components that depended on those unavailable libraries and reimplemented some of them specifically for Android [11].

We chose to process the recorded audio at a sample rate of 44100 samples per second. The TarsosDSP library lets us process real-time audio in chunks of any size we want, and we chose to process chunks of length 2048 samples, a value recommended by the TarsosDSP authors. The library also lets us set an overlap value, which is the number of samples from the end of the current chunk to carry over to the beginning of the next chunk. We chose an overlap value of 1024 samples, which was also recommended. Putting it all together, we process chunks at a rate of  $\frac{44100}{2048-1024} \approx 43$  chunks per second. This rate is more than sufficient for piano pieces, since it exceeds the the rate at which humans can even perceive separate notes.

Throughout our implementation, we aggressively strove to precompute anything we could, so that we minimize the amount of work we perform at every chunk.

### 4.1 Goertzel Algorithm

To extract the frequency magnitudes from a chunk of audio samples, one might instinctively think to use the fast Fourier transform algorithm, which extracts the discrete Fourier transform (DFT) coefficients for that chunk. These coefficients, whose absolute value would be the magnitudes, correspond to frequencies that are integer multiples of the fundamental frequency of the chunk. In our case of a sample rate of 44100 Hz and a chunk size of 2048, these frequencies are  $\frac{44100}{2048}k \approx 21.53k$  Hz, for  $k \in 0, 1, 2, \dots, 2047$ . However, few of these frequencies closely match up to the observed frequencies that we are interested in.

We decided instead to use the Goertzel algorithm [7], which computes the DFT coefficient for just a single frequency. A great property of this algorithm is that by carefully selecting parameters, we can finely home in on the frequency that we want to analyze. Namely, given positive integers  $k$  and  $N$ , and the sampling frequency  $f_s$ , the algorithm yields the DFT coefficient for the frequency  $\frac{f_s k}{N}$  Hz. Table A.1 lists the values of  $k$  and  $N$  that we use for each observed frequency. For further discussion on how we chose these values,

see Appendix B.

We specifically use a version of the Goertzel algorithm that yields the power of the frequency, which is the square of the coefficient’s magnitude. It is expressed as follows, where  $x$  is the array of sample values in the audio chunk and  $s_k$  is an intermediate array:

$$s_k[n] = x[n] + 2 \cos\left(\frac{2\pi k}{N}\right) s_k[n-1] - s_k[n-2]$$

$$|X_k|^2 = s_k[N-1]^2 - 2 \cos\left(\frac{2\pi k}{N}\right) s_k[n-1]s_k[n-2] + s_k[n-2]^2$$

We assume  $s_k[-1] = s_k[-2] = 0$ . After taking the square root of the second equation, we still need to divide by  $N$  to normalize the magnitude. Thus, the final expression for the magnitude of the frequency is:

$$\frac{\sqrt{s_k[N-1]^2 - 2 \cos\left(\frac{2\pi k}{N}\right) s_k[n-1]s_k[n-2] + s_k[n-2]^2}}{N}$$

Notice that in these expressions, we never use the value of  $k$  itself. Rather, the factor  $2 \cos\left(\frac{2\pi k}{N}\right)$  occurs twice, so it is this value we actually store for each frequency instead of  $k$ .

Ultimately, for each of the 88 observed frequencies, we apply this algorithm with the frequency’s corresponding  $k$  and  $N$  values, and putting that together gets us our magnitude vector for this audio chunk.

## 4.2 Preprocessing

When we load a music piece, we prepare several items.

First, we prepare our hidden states. If there were originally  $n$  note sets extracted from the score, then after adding the rest states, we have a total of  $2n$  hidden states:  $\{S^0, S^1, S^2, S^3, \dots, S^{2n-1}\}$

Next, we prepare a confidence array  $c$ , which is a floating-point array whose length is  $2n$ , the number of hidden states we prepared above. Each value represents the probability that the corresponding state is the current state. In other words,  $c[i] = p(S_t = S^i | \mathbf{m}_{1:t})$ . This also means that at the end of each time step, it should be the case that  $\sum_{i=0}^{2n-1} c[i] = 1$ . If the first and last states on the current page is  $S^a$  and  $S^b$ , respectively, we set the initial values of the confidence array to be  $\frac{1}{b-a+1}$  for  $c[i]$  where  $a \leq i \leq b$ .

Finally, for each of the hidden states  $S^i$ , we precompute their unit vectors  $\hat{\mathbf{S}}^i$ . Recall that this computation involves the background noise vector  $\mathbf{b}$ . To keep things simple, we assume a flat spectrum of background noise at a pretty low volume, so we let  $\mathbf{b} = \langle 0.01, 0.01, 0.01, \dots, 0.01 \rangle$ . This value should be small compared to the harmonic strengths that we characterized earlier.

With these unit vectors precomputed, it will be fast to compute the function  $E$  we designed in Section 3.2.2, since the dot product is the only thing that needs to be computed.

## 4.3 Main Loop

First, we take the chunk of audio and run it through the Goertzel algorithm to get our magnitude vector  $\mathbf{m}$ .

Recall our modified version of the forward algorithm:

$$p(S_t|\mathbf{m}_{1:t}) \propto E(\mathbf{m}_t, S_t) \sum_{S_{t-1}} p(S_t|S_{t-1})p(S_{t-1}|\mathbf{m}_{1:t-1})$$

We compute the next version of the confidence array  $c'$  for  $0 \leq i < 2n$  as follows:

$$c'[i] = E(\mathbf{m}, S^i) \sum_{j=0}^{2n-1} p(S^i|S^j)c[j]$$

After normalizing the values in  $c'$  such that  $\sum_{i=0}^{2n-1} c'[i] = 1$ , we have our new  $c$ .

At the end of each time step, we also determine which original note set  $N_i$  has the highest total confidence. Because of the associated rest state  $R_i$ , we add together their confidence values, which correspond to  $c[2i]$  and  $c[2i + 1]$ , respectively. If the note set with the highest total confidence exceeds some threshold, we report that the player is indeed located at this note set and the UI should indicate as such. Otherwise, we report that the player’s location is unknown. We experimented with different values and decided to set our confidence threshold at 0.5. In the case that the note set we report is the last one on the page, we tell the app to advance to the next page.

## 4.4 Restricting the Considered States

To follow up Section 3.3.1, we can restrict our loop if we know certain states will not get any confidence because they are too far outside of the current page. Let  $S^a$  be the earliest state we think the user might jump to (a few measures before the end of the previous page) and  $S^b$  be the latest (a few measures after the start of the next page). Instead of looping  $i$  and  $j$  from 0 to  $2n - 1$ , we can now instead loop from  $a$  to  $b$ . That way, we only consider the note sets in the current page in addition to the couple around it.

This restriction has the nice benefit of making the algorithm more scalable in terms of the number of pages in the piece. Normally, the processing complexity for one step in a hidden Markov model increases with the square of the total number of possible hidden states. However, by applying this restriction, the number of states we actually need to loop through is the number of note sets on the current page (in addition to note sets in the extra few measures before and after the page). Regardless of how many other notes exist in the rest of the piece, whether it is 20 or 2000, they are considered unreachable, so we do not need to include them in the loop.

## 4.5 Results

We ran our application on a 2012 Nexus 7 tablet, running Android 4.4.2. As of this paper, the hardware is slightly dated, but our score following algorithm performed with no perceptible latency.

We had two test pieces, *Twinkle Twinkle Little Star*, and *Minuet in G* by J.S. Bach. Both pieces were two pages long. For each, we manually specified the sequence of note sets in the score. See Appendix C for the full note set sequence of *Minuet in G*.

Our implementation works well for both pieces. When players played to the end of the first page, our app advances to the second page automatically. Additionally, it works on various pianos with slightly different

timbres. Understandably, if the instrument the player is using is not a piano, it does not follow the player as accurately, since the harmonic characteristics would be too different from the expected ones.

We found that the piano has to be fairly in tune for our algorithm to work well. If the piano is out of tune by more than about 20 cents, the Goertzel algorithm can no longer reliably extract the magnitudes of the observed frequencies.

A video of our application in action can be seen at [2].

### Minuet in G

from the 'Anna Magdalena Bach Notebook'

Moderato  
Piano  
mf  
Johann Sebastian Bach

The image shows a sheet music application interface. At the top, a dark red header contains the title 'Minuet in G' and the composer 'J.S. Bach'. Below this, the title 'Minuet in G' is displayed in a large, blue, serif font, followed by the subtitle 'from the 'Anna Magdalena Bach Notebook'' in a smaller, black, sans-serif font. The tempo 'Moderato' and the instrument 'Piano' are indicated. The music is in G major (one sharp) and 3/4 time. The score consists of four systems, each with a treble clef staff and a piano staff. Fingerings are indicated by circled numbers: 5, 3, 4, 2, 1, and 2. A red triangle points to the first measure of the second system. At the bottom, there is a red circular button with a white question mark icon, and a black navigation bar with a back arrow, a home icon, and a recent apps icon. The website 'www.makingmusicfun.net' and the copyright notice 'This arrangement copyright © 2008 www.makingmusicfun.net' are visible at the bottom of the score area.

Figure 4.1: A screenshot of the sheet music application in action. The red triangle indicates where our algorithm believes the user is currently playing.

# Chapter 5

## Future Work

### 5.1 Understanding Tempo and Rhythm

In its current form, this algorithm is completely agnostic to tempo. If the player plays the notes completely out of rhythm, as long as the notes are played in order, the algorithm does not really treat it any differently. This also means that if the piece happens to have two phrases that happen to have the same note sequence, but in a different rhythm, the algorithm still processes them the same way. This is because the resulting note set sequences for both sections would be identical.

By annotating the note sets with their lengths (half a beat, two beats, etc.), we can start to incorporate an understanding of how long we expect the note to be held. One approach could be to create a separate mechanism that keeps track of how long the player has played each note set. Since we know the number of beats each note set is supposed to last, we can estimate their current tempo, most likely with some sort of smoothing.

Using this estimated tempo, we can vary the transition probabilities over time. For example, if the user just started playing a new note set, the probability of staying on that note set is high while the probability of advancing to the next one is low. Over time, as the note set is held out, these probabilities should gradually be tipped the other way so after the expected amount of time, the probability of advancing to the next note set becomes very high.

### 5.2 Extension to other Instruments

As described in Section 3.2.1, the harmonics of note produced by an instrument can characterize that instrument's sound. By determining the harmonic characteristics for other desired instruments, we can tailor this algorithm for those as well.

This can also be implemented as a calibration process, where we have the user play a number of (possibly predetermined) notes on their instrument. We can then analyze the magnitude vectors to understand that instrument's harmonic characteristics.

## 5.3 Better Note Break Detection

At the moment, when there is a sequence of repeating notes, the algorithm has trouble telling the notes apart. Because the  $N_i \rightarrow N_i$  and  $N_i \rightarrow N_{i+1}$  transitions lead to identical-looking states in such a sequence, the forward algorithm will essentially cause the probability mass to rush towards the end of the repeated note sets.

One possible approach is to see if the magnitude of the current magnitude vector is significantly larger than that of the previous one. If so, that may indicate the onset of a new note being played. If we add this notion to observed state, we can vary the transition probabilities as necessary.

Implementing Section 5.1 may also help this problem become less severe.

## 5.4 Additional Considerations for a Useful App

We developed this algorithm as a component of a sheet music application. In order for the app to be useful, there are other issues we need to address other than just making it able to follow the user’s playing.

### 5.4.1 Importing Sheet Music

It should be easy and painless for a user to import their own sheet music. We did not have the resources to implement this import flow in our app, and thus, had to manually put together the note set sequence for the aforementioned pieces.

One of the standard formats for digital sheet music notation is MusicXML [3], which is an exportable format on modern music notation software. In principle, we could read files in this format, extract the note set sequence, and then render the pages of the score. A similar process could be done with files in ABC notation [1], which is another text format for music notation.

We could even let the user import MIDI files. While MIDI files are generally devoid of notation, such as the key, time signature, and staves, we can easily extract the sequence of notes. Then, we just render the notes on a simple score in a basic manner. It may not look as neat, but it will probably be usable.

### 5.4.2 Pagination and Page Transitions

Currently, the pagination of the score is very cut and dried. The full sequence of note sets is broken up into contiguous chunks as pages, and only one is visible at a time. While this made for a more straightforward implementation, the user experience is not optimal. As they play and get towards the end of the page, there is no way to preview the first notes on the next page without outright flipping the page themselves. Arguably, physical sheet music is no different, and the usual “workaround” is to temporarily memorize the last several measures of the current page and flip to the next one right then and there. However, since our app is digital, we have a lot more freedom and power to experiment with interactions that are not possible or very difficult on paper.

One simple way to reinvent the page flip is to present the score like a piano roll, as a single line of sheet music that horizontally stretches as much as needed. Then, the sheet music continuously slides towards the

left as the user plays the piece. This can also be done vertically, presenting the score as a single, very tall page that scrolls upward as the user plays.

Yet another way is to perform a “wipe” kind of transition. When the user approaches the end of the page, the top of the page starts to peel away, revealing the top of the next page. Once the user reaches the top of the next page, the rest of the original page peels away. This has the advantage where the notes never move within the page.

With any of these techniques, we can still apply the transition restriction optimization we discuss in Section 3.3.1, though it will not be as straightforward to implement. It is interesting to note that when we suggested these alternative page transitions to users, many of them expressed an immediate rejection of the idea. We hypothesize that this reaction may stem from years of familiarity with how they use physical sheet music. It is worth conducting a proper usability study to see if users can get accustomed to the new transitions and perhaps even prefer one over the regular page flip.

On a similar note, our implementation is currently hardcoded to advance the page only on the last note of the page. Users have expressed their desire to be able to specify where in the score they would like the page flip to happen, typically around two measures before the end of the page.

## Chapter 6

# Summary

In this paper, we have designed and implemented a hidden Markov model approach to follow a musician's location in a musical score, using only sound as input. We have demonstrated that by understanding basic sheet music semantics and how instruments produce sound, we can carefully craft the states and the probability distributions that we use in the hidden Markov model. Implementation-wise, we preprocess a lot of components so that each iteration of the main loop can run more efficiently. Ultimately, we were able to fully implement our algorithm in Java for Android devices, and it performed admirably on real pieces of music. Finally, we present various directions we can pursue in the future to further improve the robustness and accuracy of the algorithm.

# Bibliography

- [1] abc notation. <http://abcnotation.com/>.
- [2] Final presentation. <https://www.youtube.com/watch?v=itdyN98bzGI>.
- [3] Musicxml. <http://www.musicxml.com/>.
- [4] Jonathan Aceituno. Real-time score following techniques.
- [5] Andreas Arzt, Gerhard Widmer, and Simon Dixon. Automatic page turning for musicians via real-time machine listening. In *ECAI*, pages 241–245, 2008.
- [6] Simon Dixon. An on-line time warping algorithm for tracking musical performances.
- [7] Gerald Goertzel. An algorithm for the evaluation of finite trigonometric series. *American mathematical monthly*, pages 34–35, 1958.
- [8] Bryan Pardo and William Birmingham. Modeling form for on-line following of musical performances. In *PROCEEDINGS OF THE NATIONAL CONFERENCE ON ARTIFICIAL INTELLIGENCE*, volume 20, page 1018. Menlo Park, CA; Cambridge, MA; London; AAAI Press; MIT Press; 1999, 2005.
- [9] Christopher Raphael. Automatic segmentation of acoustic musical signals using hidden markov models. *Pattern Analysis and Machine Intelligence, IEEE Transactions on*, 21(4):360–370, 1999.
- [10] Christopher Raphael. A hybrid graphical model for aligning polyphonic audio with musical scores. In *ISMIR*. Citeseer, 2004.
- [11] Steve Rubin and Andrew Lee. TarsosDSP. <https://github.com/srubin/TarsosDSP>, 2014.
- [12] Joren Six, Olmo Cornelis, and Marc Leman. Tarsosdsp, a real-time audio processing framework in java. In *Audio Engineering Society Conference: 53rd International Conference: Semantic Audio*, Jan 2014.

# Appendix A

## Observed Frequencies Table

| Note Index | Note Name                        | Frequency (Hz) | Goertzel Parameters |      | Harmonic Magnitudes |       |       |       |       |       |
|------------|----------------------------------|----------------|---------------------|------|---------------------|-------|-------|-------|-------|-------|
|            |                                  |                | $k$                 | $N$  | $h_1$               | $h_2$ | $h_3$ | $h_4$ | $h_5$ | $h_6$ |
| 0          | A <sub>0</sub>                   | 27.500         | 1                   | 1604 | 0.00                | 0.00  | 5.27  | 1.12  | 6.04  | 4.68  |
| 1          | A <sub>♯0</sub> /B <sub>b0</sub> | 29.135         | 1                   | 1514 | 0.00                | 0.01  | 5.86  | 1.31  | 5.84  | 4.57  |
| 2          | B <sub>0</sub>                   | 30.868         | 1                   | 1429 | 0.00                | 0.02  | 6.45  | 1.52  | 5.65  | 4.45  |
| 3          | C <sub>1</sub>                   | 32.703         | 1                   | 1348 | 0.00                | 0.04  | 7.00  | 1.74  | 5.45  | 4.32  |
| 4          | C <sub>♯1</sub> /D <sub>b1</sub> | 34.648         | 1                   | 1273 | 0.00                | 0.08  | 7.53  | 1.96  | 5.24  | 4.19  |
| 5          | D <sub>1</sub>                   | 36.708         | 1                   | 1201 | 0.00                | 0.14  | 8.02  | 2.20  | 5.04  | 4.05  |
| 6          | D <sub>♯1</sub> /E <sub>b1</sub> | 38.891         | 1                   | 1134 | 0.01                | 0.24  | 8.46  | 2.44  | 4.83  | 3.91  |
| 7          | E <sub>1</sub>                   | 41.203         | 1                   | 1070 | 0.01                | 0.40  | 8.85  | 2.69  | 4.63  | 3.77  |
| 8          | F <sub>1</sub>                   | 43.654         | 2                   | 2020 | 0.02                | 0.62  | 9.19  | 2.93  | 4.42  | 3.62  |
| 9          | F <sub>♯1</sub> /G <sub>b1</sub> | 46.249         | 2                   | 1907 | 0.03                | 0.94  | 9.46  | 3.17  | 4.22  | 3.47  |
| 10         | G <sub>1</sub>                   | 48.999         | 2                   | 1800 | 0.05                | 1.37  | 9.68  | 3.41  | 4.02  | 3.32  |
| 11         | G <sub>♯1</sub> /A <sub>b1</sub> | 51.913         | 2                   | 1699 | 0.07                | 1.93  | 9.83  | 3.64  | 3.83  | 3.18  |
| 12         | A <sub>1</sub>                   | 55.000         | 2                   | 1604 | 0.10                | 2.65  | 9.92  | 3.85  | 3.64  | 3.03  |
| 13         | A <sub>♯1</sub> /B <sub>b1</sub> | 58.270         | 2                   | 1514 | 0.15                | 3.54  | 9.94  | 4.06  | 3.45  | 2.88  |
| 14         | B <sub>1</sub>                   | 61.735         | 2                   | 1429 | 0.21                | 4.61  | 9.91  | 4.25  | 3.27  | 2.74  |
| 15         | C <sub>2</sub>                   | 65.406         | 3                   | 2023 | 0.29                | 5.85  | 9.82  | 4.42  | 3.10  | 2.60  |
| 16         | C <sub>♯2</sub> /D <sub>b2</sub> | 69.296         | 3                   | 1909 | 0.39                | 7.26  | 9.69  | 4.57  | 2.93  | 2.46  |
| 17         | D <sub>2</sub>                   | 73.416         | 3                   | 1802 | 0.53                | 8.82  | 9.50  | 4.71  | 2.76  | 2.33  |
| 18         | D <sub>♯2</sub> /E <sub>b2</sub> | 77.782         | 3                   | 1701 | 0.70                | 10.50 | 9.27  | 4.82  | 2.60  | 2.20  |
| 19         | E <sub>2</sub>                   | 82.407         | 3                   | 1605 | 0.90                | 12.26 | 9.00  | 4.91  | 2.45  | 2.07  |
| 20         | F <sub>2</sub>                   | 87.307         | 4                   | 2020 | 1.16                | 14.05 | 8.70  | 4.98  | 2.31  | 1.95  |
| 21         | F <sub>♯2</sub> /G <sub>b2</sub> | 92.499         | 4                   | 1907 | 1.47                | 15.82 | 8.37  | 5.03  | 2.17  | 1.83  |
| 22         | G <sub>2</sub>                   | 97.999         | 4                   | 1800 | 1.83                | 17.51 | 8.02  | 5.05  | 2.03  | 1.72  |
| 23         | G <sub>♯2</sub> /A <sub>b2</sub> | 103.826        | 4                   | 1699 | 2.26                | 19.08 | 7.65  | 5.06  | 1.90  | 1.61  |

Continued on next page

Table A.1 – continued from previous page

| Note Index | Note Name                                                | Frequency (Hz) | Goertzel Parameters |      | Harmonic Magnitudes |       |       |       |       |       |
|------------|----------------------------------------------------------|----------------|---------------------|------|---------------------|-------|-------|-------|-------|-------|
|            |                                                          |                | $k$                 | $N$  | $h_1$               | $h_2$ | $h_3$ | $h_4$ | $h_5$ | $h_6$ |
| 24         | A <sub>2</sub>                                           | 110.000        | 5                   | 2005 | 2.76                | 20.45 | 7.27  | 5.04  | 1.78  | 1.51  |
| 25         | A <sub>2</sub> <sup>#</sup> /B <sub>2</sub> <sup>b</sup> | 116.541        | 5                   | 1892 | 3.32                | 21.60 | 6.88  | 5.00  | 1.67  | 1.41  |
| 26         | B <sub>2</sub>                                           | 123.471        | 5                   | 1786 | 3.95                | 22.49 | 6.49  | 4.94  | 1.56  | 1.32  |
| 27         | C <sub>3</sub>                                           | 130.813        | 6                   | 2023 | 4.66                | 23.09 | 6.09  | 4.87  | 1.45  | 1.23  |
| 28         | C <sub>3</sub> <sup>#</sup> /D <sub>3</sub> <sup>b</sup> | 138.591        | 6                   | 1909 | 5.43                | 23.38 | 5.70  | 4.78  | 1.36  | 1.15  |
| 29         | D <sub>3</sub>                                           | 146.832        | 6                   | 1802 | 6.26                | 23.37 | 5.32  | 4.67  | 1.26  | 1.07  |
| 30         | D <sub>3</sub> <sup>#</sup> /E <sub>3</sub> <sup>b</sup> | 155.563        | 7                   | 1984 | 7.16                | 23.07 | 4.94  | 4.55  | 1.17  | 0.99  |
| 31         | E <sub>3</sub>                                           | 164.814        | 7                   | 1873 | 8.10                | 22.49 | 4.58  | 4.41  | 1.09  | 0.92  |
| 32         | F <sub>3</sub>                                           | 174.614        | 8                   | 2020 | 9.08                | 21.67 | 4.23  | 4.27  | 1.01  | 0.85  |
| 33         | F <sub>3</sub> <sup>#</sup> /G <sub>3</sub> <sup>b</sup> | 184.997        | 8                   | 1907 | 10.09               | 20.63 | 3.89  | 4.12  | 0.94  | 0.79  |
| 34         | G <sub>3</sub>                                           | 195.998        | 9                   | 2025 | 11.12               | 19.43 | 3.57  | 3.96  | 0.87  | 0.73  |
| 35         | G <sub>3</sub> <sup>#</sup> /A <sub>3</sub> <sup>b</sup> | 207.652        | 9                   | 1911 | 12.14               | 18.10 | 3.26  | 3.79  | 0.81  | 0.68  |
| 36         | A <sub>3</sub>                                           | 220.000        | 10                  | 2005 | 13.15               | 16.68 | 2.98  | 3.63  | 0.75  | 0.62  |
| 37         | A <sub>3</sub> <sup>#</sup> /B <sub>3</sub> <sup>b</sup> | 233.082        | 10                  | 1892 | 14.13               | 15.21 | 2.71  | 3.45  | 0.69  | 0.57  |
| 38         | B <sub>3</sub>                                           | 246.942        | 11                  | 1964 | 15.07               | 13.73 | 2.46  | 3.28  | 0.64  | 0.53  |
| 39         | C <sub>4</sub>                                           | 261.626        | 12                  | 2023 | 15.94               | 12.28 | 2.22  | 3.11  | 0.59  | 0.49  |
| 40         | C <sub>4</sub> <sup>#</sup> /D <sub>4</sub> <sup>b</sup> | 277.183        | 12                  | 1909 | 16.73               | 10.87 | 2.00  | 2.93  | 0.54  | 0.45  |
| 41         | D <sub>4</sub>                                           | 293.665        | 13                  | 1952 | 17.44               | 9.53  | 1.80  | 2.76  | 0.50  | 0.41  |
| 42         | D <sub>4</sub> <sup>#</sup> /E <sub>4</sub> <sup>b</sup> | 311.127        | 14                  | 1984 | 18.05               | 8.29  | 1.62  | 2.60  | 0.46  | 0.38  |
| 43         | E <sub>4</sub>                                           | 329.628        | 15                  | 2007 | 18.55               | 7.14  | 1.45  | 2.43  | 0.42  | 0.35  |
| 44         | F <sub>4</sub>                                           | 349.228        | 16                  | 2020 | 18.93               | 6.09  | 1.29  | 2.27  | 0.39  | 0.32  |
| 45         | F <sub>4</sub> <sup>#</sup> /G <sub>4</sub> <sup>b</sup> | 369.994        | 17                  | 2026 | 19.19               | 5.16  | 1.15  | 2.12  | 0.36  | 0.29  |
| 46         | G <sub>4</sub>                                           | 391.995        | 18                  | 2025 | 19.32               | 4.33  | 1.02  | 1.97  | 0.33  | 0.27  |
| 47         | G <sub>4</sub> <sup>#</sup> /A <sub>4</sub> <sup>b</sup> | 415.305        | 19                  | 2018 | 19.33               | 3.60  | 0.90  | 1.83  | 0.30  | 0.24  |
| 48         | A <sub>4</sub>                                           | 440.000        | 20                  | 2005 | 19.22               | 2.98  | 0.80  | 1.69  | 0.28  | 0.22  |
| 49         | A <sub>4</sub> <sup>#</sup> /B <sub>4</sub> <sup>b</sup> | 466.164        | 21                  | 1987 | 18.99               | 2.44  | 0.70  | 1.56  | 0.25  | 0.20  |
| 50         | B <sub>4</sub>                                           | 493.883        | 22                  | 1964 | 18.65               | 1.98  | 0.62  | 1.44  | 0.23  | 0.18  |
| 51         | C <sub>5</sub>                                           | 523.251        | 24                  | 2023 | 18.21               | 1.60  | 0.54  | 1.32  | 0.21  | 0.17  |
| 52         | C <sub>5</sub> <sup>#</sup> /D <sub>5</sub> <sup>b</sup> | 554.365        | 25                  | 1989 | 17.67               | 1.28  | 0.48  | 1.21  | 0.19  | 0.15  |
| 53         | D <sub>5</sub>                                           | 587.330        | 27                  | 2027 | 17.06               | 1.02  | 0.42  | 1.11  | 0.18  | 0.14  |
| 54         | D <sub>5</sub> <sup>#</sup> /E <sub>5</sub> <sup>b</sup> | 622.254        | 28                  | 1984 | 16.37               | 0.80  | 0.36  | 1.01  | 0.16  | 0.13  |
| 55         | E <sub>5</sub>                                           | 659.255        | 30                  | 2007 | 15.62               | 0.63  | 0.32  | 0.92  | 0.15  | 0.11  |
| 56         | F <sub>5</sub>                                           | 698.456        | 32                  | 2020 | 14.82               | 0.49  | 0.28  | 0.84  | 0.13  | 0.10  |
| 57         | F <sub>5</sub> <sup>#</sup> /G <sub>5</sub> <sup>b</sup> | 739.989        | 34                  | 2026 | 13.99               | 0.38  | 0.24  | 0.76  | 0.12  | n/a   |
| 58         | G <sub>5</sub>                                           | 783.991        | 36                  | 2025 | 13.14               | 0.29  | 0.21  | 0.69  | 0.11  | n/a   |
| 59         | G <sub>5</sub> <sup>#</sup> /A <sub>5</sub> <sup>b</sup> | 830.609        | 38                  | 2018 | 12.27               | 0.22  | 0.18  | 0.62  | 0.10  | n/a   |

Continued on next page

Table A.1 – continued from previous page

| Note Index | Note Name                                                | Frequency (Hz) | Goertzel Parameters |      | Harmonic Magnitudes |       |       |       |       |       |
|------------|----------------------------------------------------------|----------------|---------------------|------|---------------------|-------|-------|-------|-------|-------|
|            |                                                          |                | $k$                 | $N$  | $h_1$               | $h_2$ | $h_3$ | $h_4$ | $h_5$ | $h_6$ |
| 60         | A <sub>5</sub>                                           | 880.000        | 40                  | 2005 | 11.41               | 0.17  | 0.15  | 0.56  | n/a   | n/a   |
| 61         | A <sub>5</sub> <sup>#</sup> /B <sub>5</sub> <sup>b</sup> | 932.328        | 43                  | 2034 | 10.55               | 0.13  | 0.13  | 0.51  | n/a   | n/a   |
| 62         | B <sub>5</sub>                                           | 987.767        | 45                  | 2009 | 9.71                | 0.09  | 0.11  | 0.46  | n/a   | n/a   |
| 63         | C <sub>6</sub>                                           | 1046.502       | 48                  | 2023 | 8.89                | 0.07  | 0.10  | 0.41  | n/a   | n/a   |
| 64         | C <sub>6</sub> <sup>#</sup> /D <sub>6</sub> <sup>b</sup> | 1108.731       | 51                  | 2029 | 8.10                | 0.05  | 0.08  | n/a   | n/a   | n/a   |
| 65         | D <sub>6</sub>                                           | 1174.659       | 54                  | 2027 | 7.35                | 0.04  | 0.07  | n/a   | n/a   | n/a   |
| 66         | D <sub>6</sub> <sup>#</sup> /E <sub>6</sub> <sup>b</sup> | 1244.508       | 57                  | 2020 | 6.63                | 0.03  | 0.06  | n/a   | n/a   | n/a   |
| 67         | E <sub>6</sub>                                           | 1318.510       | 61                  | 2040 | 5.96                | 0.02  | 0.05  | n/a   | n/a   | n/a   |
| 68         | F <sub>6</sub>                                           | 1396.913       | 64                  | 2020 | 5.33                | 0.01  | 0.04  | n/a   | n/a   | n/a   |
| 69         | F <sub>6</sub> <sup>#</sup> /G <sub>6</sub> <sup>b</sup> | 1479.978       | 68                  | 2026 | 4.75                | 0.01  | n/a   | n/a   | n/a   | n/a   |
| 70         | G <sub>6</sub>                                           | 1567.982       | 72                  | 2025 | 4.21                | 0.01  | n/a   | n/a   | n/a   | n/a   |
| 71         | G <sub>6</sub> <sup>#</sup> /A <sub>6</sub> <sup>b</sup> | 1661.219       | 77                  | 2044 | 3.72                | 0.01  | n/a   | n/a   | n/a   | n/a   |
| 72         | A <sub>6</sub>                                           | 1760.000       | 81                  | 2030 | 3.27                | 0.00  | n/a   | n/a   | n/a   | n/a   |
| 73         | A <sub>6</sub> <sup>#</sup> /B <sub>6</sub> <sup>b</sup> | 1864.655       | 86                  | 2034 | 2.86                | 0.00  | n/a   | n/a   | n/a   | n/a   |
| 74         | B <sub>6</sub>                                           | 1975.533       | 91                  | 2031 | 2.50                | 0.00  | n/a   | n/a   | n/a   | n/a   |
| 75         | C <sub>7</sub>                                           | 2093.005       | 97                  | 2044 | 2.17                | 0.00  | n/a   | n/a   | n/a   | n/a   |
| 76         | C <sub>7</sub> <sup>#</sup> /D <sub>7</sub> <sup>b</sup> | 2217.461       | 102                 | 2029 | 1.87                | n/a   | n/a   | n/a   | n/a   | n/a   |
| 77         | D <sub>7</sub>                                           | 2349.318       | 109                 | 2046 | 1.61                | n/a   | n/a   | n/a   | n/a   | n/a   |
| 78         | D <sub>7</sub> <sup>#</sup> /E <sub>7</sub> <sup>b</sup> | 2489.016       | 115                 | 2038 | 1.38                | n/a   | n/a   | n/a   | n/a   | n/a   |
| 79         | E <sub>7</sub>                                           | 2637.020       | 122                 | 2040 | 1.18                | n/a   | n/a   | n/a   | n/a   | n/a   |
| 80         | F <sub>7</sub>                                           | 2793.826       | 129                 | 2036 | 1.01                | n/a   | n/a   | n/a   | n/a   | n/a   |
| 81         | F <sub>7</sub> <sup>#</sup> /G <sub>7</sub> <sup>b</sup> | 2959.955       | 137                 | 2041 | 0.85                | n/a   | n/a   | n/a   | n/a   | n/a   |
| 82         | G <sub>7</sub>                                           | 3135.963       | 145                 | 2039 | 0.72                | n/a   | n/a   | n/a   | n/a   | n/a   |
| 83         | G <sub>7</sub> <sup>#</sup> /A <sub>7</sub> <sup>b</sup> | 3322.438       | 154                 | 2044 | 0.61                | n/a   | n/a   | n/a   | n/a   | n/a   |
| 84         | A <sub>7</sub>                                           | 3520.000       | 163                 | 2042 | 0.51                | n/a   | n/a   | n/a   | n/a   | n/a   |
| 85         | A <sub>7</sub> <sup>#</sup> /B <sub>7</sub> <sup>b</sup> | 3729.310       | 173                 | 2046 | 0.43                | n/a   | n/a   | n/a   | n/a   | n/a   |
| 86         | B <sub>7</sub>                                           | 3951.066       | 183                 | 2043 | 0.35                | n/a   | n/a   | n/a   | n/a   | n/a   |
| 87         | C <sub>8</sub>                                           | 4186.009       | 194                 | 2044 | 0.29                | n/a   | n/a   | n/a   | n/a   | n/a   |

## Appendix B

# Computing $N$ and $k$ for each Observed Frequency

Mathematically speaking, given a positive integer  $N$  and a positive integer  $k$ , the Goertzel algorithm computes the  $k$ th coefficient of an  $N$ -sample discrete Fourier transform. For us, using our sample rate of 44100 Hz, this means that the algorithm will yield the coefficient for the frequency  $f = \frac{44100k}{N}$  Hz. Thus, our goal is that for each one of our observed frequencies  $f_0$ , we want to find integers  $k$  and  $N$  such that  $\frac{44100k}{N}$  is as close to  $f_0$  as possible. Rearranging our equation yields:

$$\begin{aligned}\frac{44100k}{N} &= f \\ k &= \frac{N}{44100}f\end{aligned}$$

Because our chunk size is 2048, that is all the samples we have available, so  $N$  has to be 2048 or less. Thus, we first plug in 2048 for  $N$  and our desired frequency  $f_0$  into  $f$ , and then round  $k$  down to the nearest integer. Then, we compute  $N$  by plugging in our new  $k$  back into the equation and rounding the result.

$$\begin{aligned}k &= \left\lfloor \frac{2048}{44100}f_0 \right\rfloor \\ N &= \text{round}\left(\frac{44100k}{f_0}\right)\end{aligned}$$

Over all the observed frequencies, the greatest relative error between the resulting frequency  $\frac{44100k}{N}$  and the target frequency  $f_0$  is 0.0365%, so the precision we can attain is very high.

As an aside, notice how the for the lowest note  $A_0$ ,  $k = 1$  and  $N = 1604$ . This implies that our chunk size must be at least 1604 samples in order to accurately capture the magnitude of that corresponding frequency. In other words, with any fewer samples, there simply would not be enough samples to represent one period of 27.5 Hz. This minimum chunk size is one of the reasons why we chose a chunk size of 2048 samples.

# Appendix C

## *Minuet in G* Note Sets

|                               |                              |                               |                                |                                |
|-------------------------------|------------------------------|-------------------------------|--------------------------------|--------------------------------|
| $N_0 = \{G_3, B_3, D_5\}$     | $N_{28} = \{A_4\}$           | $N_{56} = \{C_5\}$            | $N_{84} = \{E_3, G_5\}$        | $N_{112} = \{F\sharp_4\}$      |
| $N_1 = \{G_4\}$               | $N_{29} = \{G_3, B_4\}$      | $N_{57} = \{F\sharp_3, B_4\}$ | $N_{85} = \{D_5\}$             | $N_{113} = \{C_4, G_4\}$       |
| $N_2 = \{A_4\}$               | $N_{30} = \{G_4\}$           | $N_{58} = \{A_4\}$            | $N_{86} = \{A_3, C\sharp_5\}$  | $N_{114} = \{B_3, D_5\}$       |
| $N_3 = \{A_3, B_4\}$          | $N_{31} = \{D_4, B_4\}$      | $N_{59} = \{G_3, B_4\}$       | $N_{87} = \{B_4\}$             | $N_{115} = \{A_3, C_5\}$       |
| $N_4 = \{C_5\}$               | $N_{32} = \{D_3, A_4\}$      | $N_{60} = \{C_5\}$            | $N_{88} = \{C_5\}$             | $N_{116} = \{G_3, B_4\}$       |
| $N_5 = \{B_3, D_5\}$          | $N_{33} = \{C_4\}$           | $N_{61} = \{B_4\}$            | $N_{89} = \{A_2, A_4\}$        | $N_{117} = \{D_4, A_4\}$       |
| $N_6 = \{G_4\}$               | $N_{34} = \{B_3\}$           | $N_{62} = \{B_3, A_4\}$       | $N_{90} = \{A_3, A_4\}$        | $N_{118} = \{G_4\}$            |
| $N_7 = \{G_4\}$               | $N_{35} = \{A_3\}$           | $N_{63} = \{G_4\}$            | $N_{91} = \{B_4\}$             | $N_{119} = \{F\sharp_4\}$      |
| $N_8 = \{C_4, E_5\}$          | $N_{36} = \{G_3, B_3, D_5\}$ | $N_{64} = \{C_4, A_4\}$       | $N_{92} = \{C\sharp_5\}$       | $N_{120} = \{G_4\}$            |
| $N_9 = \{C_5\}$               | $N_{37} = \{G_4\}$           | $N_{65} = \{D_4, B_4\}$       | $N_{93} = \{D_5\}$             | $N_{121} = \{A_4\}$            |
| $N_{10} = \{D_5\}$            | $N_{38} = \{A_4\}$           | $N_{66} = \{A_4\}$            | $N_{94} = \{E_5\}$             | $N_{122} = \{D_3, D_4\}$       |
| $N_{11} = \{E_5\}$            | $N_{39} = \{A_3, B_4\}$      | $N_{67} = \{D_3, G_4\}$       | $N_{95} = \{F\sharp_5\}$       | $N_{123} = \{E_4\}$            |
| $N_{12} = \{F\sharp_5\}$      | $N_{40} = \{C_5\}$           | $N_{68} = \{F\sharp_4\}$      | $N_{96} = \{B_3, G_5\}$        | $N_{124} = \{F\sharp_4\}$      |
| $N_{13} = \{B_3, G_5\}$       | $N_{41} = \{G_3, D_5\}$      | $N_{69} = \{G_3, G_4\}$       | $N_{97} = \{D_4, F\sharp_5\}$  | $N_{125} = \{G_4\}$            |
| $N_{14} = \{G_4\}$            | $N_{42} = \{B_3, G_4\}$      | $N_{70} = \{G_2\}$            | $N_{98} = \{C\sharp_4, E_5\}$  | $N_{126} = \{F\sharp_3, A_4\}$ |
| $N_{15} = \{G_4\}$            | $N_{43} = \{G_3, G_4\}$      | $N_{71} = \{G_3, B_5\}$       | $N_{99} = \{D_4, F\sharp_5\}$  | $N_{127} = \{B_4\}$            |
| $N_{16} = \{A_3, C_5\}$       | $N_{44} = \{C_4, E_5\}$      | $N_{72} = \{G_5\}$            | $N_{100} = \{F\sharp_3, A_4\}$ | $N_{128} = \{E_3, C_5\}$       |
| $N_{17} = \{D_5\}$            | $N_{45} = \{C_5\}$           | $N_{73} = \{A_5\}$            | $N_{101} = \{A_3, C\sharp_5\}$ | $N_{129} = \{G_3, B_4\}$       |
| $N_{18} = \{C_5\}$            | $N_{46} = \{D_5\}$           | $N_{74} = \{B_5\}$            | $N_{102} = \{D_4, D_5\}$       | $N_{130} = \{F\sharp_3, A_4\}$ |
| $N_{19} = \{B_4\}$            | $N_{47} = \{E_5\}$           | $N_{75} = \{G_5\}$            | $N_{103} = \{D_4, D_5\}$       | $N_{131} = \{G_3, B_4\}$       |
| $N_{20} = \{A_4\}$            | $N_{48} = \{F\sharp_5\}$     | $N_{76} = \{F\sharp_3, A_5\}$ | $N_{104} = \{D_3\}$            | $N_{132} = \{D_5\}$            |
| $N_{21} = \{G_3, B_4\}$       | $N_{49} = \{B_3, G_5\}$      | $N_{77} = \{D_5\}$            | $N_{105} = \{C_4\}$            | $N_{133} = \{B_2, G_4\}$       |
| $N_{22} = \{C_5\}$            | $N_{50} = \{C_4, G_4\}$      | $N_{78} = \{E_5\}$            | $N_{106} = \{B_3, D_5\}$       | $N_{134} = \{D_3, F\sharp_4\}$ |
| $N_{23} = \{B_4\}$            | $N_{51} = \{B_3\}$           | $N_{79} = \{F\sharp_5\}$      | $N_{107} = \{D_4, G_4\}$       | $N_{135} = \{G_3, B_3, G_4\}$  |
| $N_{24} = \{A_4\}$            | $N_{52} = \{A_3, G_4\}$      | $N_{80} = \{D_5\}$            | $N_{108} = \{F\sharp_4\}$      | $N_{136} = \{D_3, B_3\}$       |
| $N_{25} = \{G_4\}$            | $N_{53} = \{G_3\}$           | $N_{81} = \{E_3, G_5\}$       | $N_{109} = \{B_3, G_4\}$       | $N_{137} = \{G_2\}$            |
| $N_{26} = \{D_4, F\sharp_4\}$ | $N_{54} = \{A_3, C_5\}$      | $N_{82} = \{G_3, E_5\}$       | $N_{110} = \{C_4, E_5\}$       |                                |
| $N_{27} = \{B_3, G_4\}$       | $N_{55} = \{D_5\}$           | $N_{83} = \{F\sharp_5\}$      | $N_{111} = \{E_4, G_4\}$       |                                |